Modeling of Point Defect Kinetics During Thermal Oxidation

M.Budil, W.Jüngling, E.Guerrero, S.Selberherr, H.Pötzl

Institut für Allgemeine Elektrotechnik und Elektronik
Technical University of Vienna
Gußhausstraße 27-29, 1040-Vienna, AUSTRIA
and
Ludwig Boltzmann-Institut für Festkörperphysik,
Kopernikusgasse 5, Vienna, Austria

ABSTRACT: This work presents the modeling of the kinetics of interstitial supersaturation and vacancy undersaturation during thermal oxidation of silicon. Furthermore the time dependence of the interstitial supersaturation at the silicon surface is investigated. The influence of the surface recombination velocity and the bulk recombination on the behaviour of point defects is examined.

1. INTRODUCTION

The shrinkage of devices in modern integrated circuits requires a better understanding of the critical process steps in the silicon VLSI-technology. Silicon point defects such as vacancies (V) and interstitials (I) influence significantly the dopant diffusion during the thermal oxidation. The generation and recombination of these defects requires therefore accurate modeling in the bulk as well as at the surfaces of the wafer. Recently many publications have treated the oxidation enhanced and retarded diffusion (OED/ORD) of the most common dopants in silicon /1,2,3/. A main problem in studying OED/ORD phenomena is the little knowledge about the correlation between the different processes during the thermal oxidation such as recombination, generation and diffusion of the point defects.

The numerical simulation is an important tool for the study and comprehension of point defect kinetics. The simulations impose a high degree of flexibility on the process simulator since various systems of partial differential equations must be evaluated during the investigations.

The aim of this work is to describe the behaviour of

point defects during thermal oxidation and the dependence of this behaviour on the parameter values.

2. NUMERICAL SIMULATION

In this work the program package ZOMBIE was used. ZOMBIE is a one-dimensional general solver for systems of coupled parabolic, elliptic and ordinary differential equations with non constant coefficients. ZOMBIE has been designed for the simulation of complete IC-fabrication steps and the determination of the electric behaviour of these devices. Equations (1) and (2) define the system of n coupled partial differential equations which can be solved by ZOMBIE with the general boundary conditions (3).

$$\sum_{j=1}^{n} a_{ij} \cdot \frac{\partial c_j}{\partial t} + \frac{\partial J_i}{\partial x} = G_i - R_i \qquad (1)$$

$$J_i = \sum_{j=1}^{n} D_{ij} \cdot \frac{\partial c_j}{\partial x} \pm \sum_{j=1}^{n} \mu_{ij} \cdot c_j \cdot \frac{\partial \psi}{\partial x} \qquad (2)$$

$$\sum_{j=1}^{n} \xi_{ij} \cdot c_j + \sum_{j=1}^{n} \eta_{ij} \cdot J_j = F_i \qquad (3)$$

To begin with we discuss the model of the interstitial supersaturation proposed by Hu /4/ and at the same time we compare the analytical solution of this model with the numerical solution of ZOMBIE.

2.1 Analytical Solution

The generation of I (G_I) is accepted to be proportional to the oxidation rate of silicon. According to the oxidation model of Grove /5/ this rate is (linear oxidation regime) constant for short oxidation times and then has a dependence of $t^{-1/2}$ on the oxidation time (t) (parabolic oxidation regime). In /4/ G_I at the $Si\text{-}SiO_2$-interface is given by

$$G_I = A \cdot t^{-\frac{1}{2}} \qquad (4)$$

The high diffusivity of interstitials requires in addition the solution of the continuity equation within the whole wafer.

$$\frac{\partial c_I}{\partial t} = D_I \cdot \frac{\partial^2 c_I}{\partial x^2} \qquad (5)$$

D_I and C_I denote the diffusion coefficient and the concentration of I, x the depth in the bulk. The initial and boundary conditions are given by

$$C_I = C_I^{eq} \qquad t=0 \qquad (6.a)$$

$$J_I = G_I - K_I \cdot (C_I - C_I^{eq}) \qquad x=0,\ t>0 \qquad (6.b)$$

$$C_I^{eq} = C \qquad x=\infty,\ t>0 \qquad (6.c)$$

C_I^{eq} denotes the thermodynamic equilibrium concentration of interstitials. The Si/SiO_2-interface is localized at x=0. The first term on the right side of (6.b) describes the generation of interstitials and the second term the recombination of I at the interface with K_I as a constant factor, which denotes the surface recombination velocity of the interstitials. The analytical solution of equations (4) to (6) is given in /4/.

$$C(x,t) = A \cdot \sqrt{\frac{\pi}{D_I}} \cdot \exp(-\lambda^2 + (\sqrt{\tau}+\lambda)^2) \cdot \operatorname{erfc}(\sqrt{\tau}+\lambda) + C_I^{eq} \qquad (7)$$

where λ and τ are normalized parameters

$$\lambda = \frac{x}{2\sqrt{D_I t}} \qquad (8.a)$$

$$\tau = \frac{t \cdot K_I^2}{D_I} \qquad (8.b)$$

If G_I is constant one obtains

$$C_I(\lambda,\tau) = C_I^{eq} + G_I/K_I \cdot (\operatorname{erfc}(\lambda) - e^{2\lambda\sqrt{\tau}+\tau} \cdot \operatorname{erfc}(\lambda+\sqrt{\tau})) \qquad (9)$$

The interstitial supersaturation influences the growth of stacking faults (OSF) and the diffusion of dopants (OED/ORD). Therefore these experiments permit an insight into the behaviour of average interstitial supersaturation. The average supersaturation is defined by

$$\langle \Delta C_I \rangle = \frac{1}{t} \cdot \int_0^t \left(\frac{C_I}{C_I^{eq}} - 1 \right) d\tau \qquad (10)$$

For the average interstitial concentration we obtain by inserting (10) in (7) and (9)

$$\langle \Delta C_I \rangle = G_I/(K_I \cdot \tau) \cdot ((\tau+2\lambda^2\tau+2\lambda\sqrt{\tau}+1) \cdot \mathrm{erfc}(\lambda) - -2/\sqrt{\pi} \cdot (\lambda\tau+\sqrt{\tau}) \cdot e^{-\lambda^2} - e^{2\lambda\sqrt{\tau}+\tau} \cdot \mathrm{erfc}(\lambda+\sqrt{\tau})) \qquad (11)$$

$$\langle \Delta C_I \rangle = A/(C_I^{eq} \cdot \tau) \cdot (\pi/D_I)^{1/2} \cdot (e^{\tau+2\lambda\sqrt{\tau}} \cdot \mathrm{erfc}(\lambda+\sqrt{\tau}) + 2 \cdot (\tau/\pi)^{1/2} \cdot e^{-\lambda^2} - (2\lambda\sqrt{\tau}+1) \cdot \mathrm{erfc}(\lambda)) \qquad (12)$$

Equation (11) is valid for the linear and (12) for the parabolic oxidation regime. The next step is to compare the analytical solutions (7), (9), (11) and (12) with the corresponding numerical solutions of ZOMBIE.

2.2 The Numerical Solution

Equation (5) was solved numerically using the initial condition in (6). Further the diffusion was simulated in a 150µm layer. The boundary conditions (3) are the following:

$$J_I = G_I - K_I \cdot (C_I - C_I^{eq}) \qquad x=0,\ t>0 \qquad (13.a)$$

$$J_I = 0 \qquad x=150\mu m,\ t>0 \qquad (13.b)$$

For the numerical computation of $\langle \Delta C_I \rangle$ with ZOMBIE equation (10) was transformed to

$$t \cdot \frac{\partial \langle \Delta C_I \rangle}{\partial t} = \frac{C_I^{eq}}{C_I} - 1 - \langle \Delta C_I \rangle \qquad (14)$$

For (14) the following initial condition was used

$$\langle \Delta C_I \rangle = 0 \qquad (15)$$

The values of the different parameters are given in table 1.

TABLE 1

Parameter values for the numerical simulation /6/

G_I	$= 10^{14}$ cm^{-2}sec^{-1} (linear rate)
A	$= 10^{14}$ cm^{-2}sec$^{-1/2}$ (parabolic rate)
D_I	$= 10^{-6}$ cm^{-2}sec^{-1}
C_I^{eq}	$= 10^{14}$ cm^{-3}
K_I	$= 5.10^{-3}$ cm·sec^{-1}

The parabolic generation term is singular at t=0 and therfore a starting time of 10^{-11} sec was chosen.

2.3 Comparision of the Analytical and Numerical Solution

The Fig.1 and Fig.2 show the numerical and analytical solution of C_I and of the average supersaturation for the linear oxidation rate, Fig.3 and Fig.4 for the parabolic one. The simulation time was chosen lower or equal 10 sec because interstitials reach the backside of the wafer after this time and the analytical solution becomes invalid.

We define the error between the analytical and numerical solution as

$$\text{ERROR} = \frac{C_I^{num} - C_I^{ana}}{C_I^{ana}} \cdot 100\% \qquad (16)$$

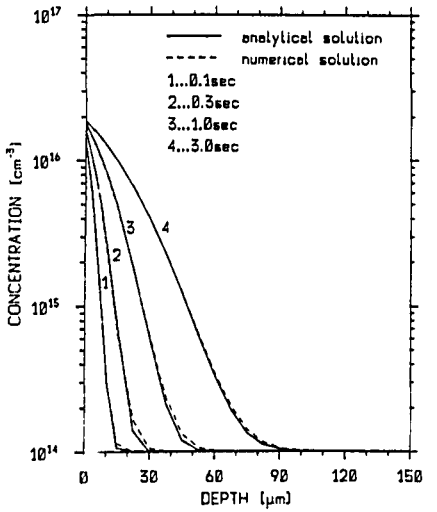

Fig.1

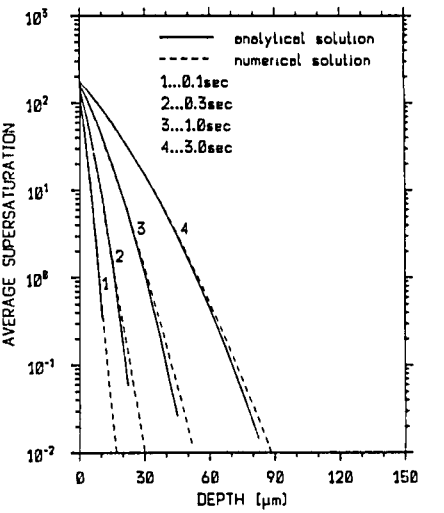

Fig.2

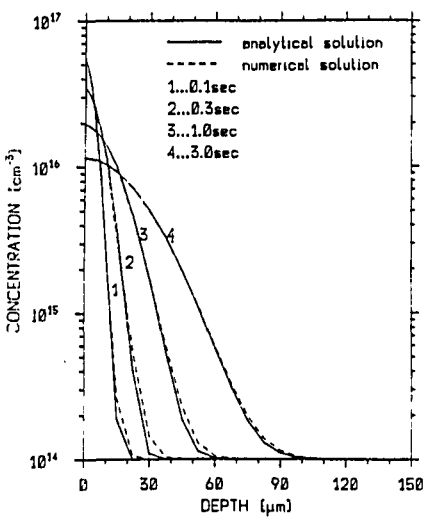

Fig.3

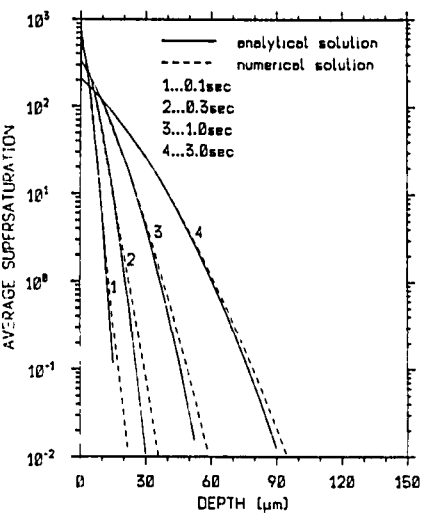

Fig.4

Fig.5 to Fig.8 show this error for different depths of the bulk. The error of 50% and more in the upper curves shows a considerable deviation from the numerical solution. Yet this results from the definition of the error; with respect to the absolute values the numerical solution is very close to the analytical solution.

The next section shows the simulation of C_I and $\langle \Delta C_I \rangle$ by a physical model for G_I. In addition a more accurate model for the growth rate of the oxide is chosen than the equation of Grove /5/.

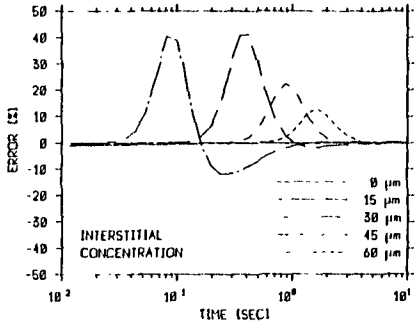

Fig.5

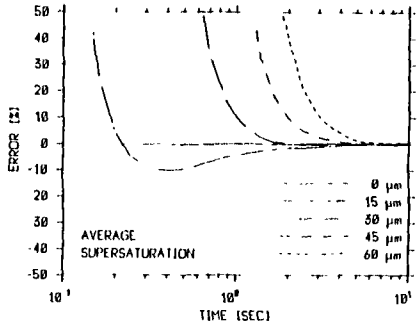

Fig.6

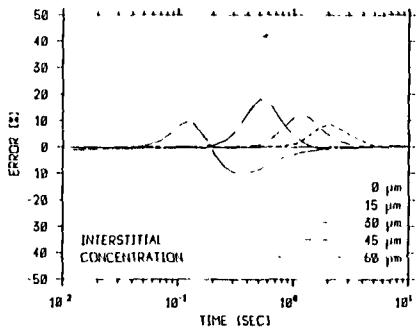

Fig.7

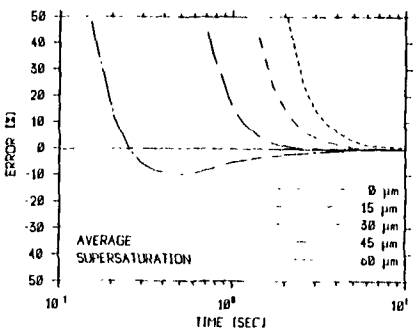

Fig.8

3.GENERATION OF INTERSTITIALS

3.1 The Oxidation Growth Rate

In this work the model of Massoud /7/ is used.

$$\frac{\partial X_{ox}}{\partial t} = \frac{B}{2 \cdot X_{ox} + A} + C_1 \cdot e^{-\frac{X_{ox}}{L_1}} + C_2 \cdot e^{-\frac{X_{ox}}{L_2}} \qquad (17)$$

This equation describes the growth rate as a function of thickness. X_{ox} is the oxide thickness and the coefficients B and B/A are the parabolic and linear rate constants. Further the coefficients L_1, L_2 C_1 and C_2 are constants and given in table 2.

TABLE 2

Parameter values for the thermal oxidation of silicon and diffusion of interstitials at 1000°C /7,8/.

B/A	$= 0.0132\ nm.sec^{-1}$
B	$= 4.68\ nm^2.sec^{-1}$
C_1	$= 0.083\ nm.sec^{-1}$
L_1	$= 1.24\ nm$
C_D2	$= 0.0452\ nm.sec^{-1}$
L_2	$= 6.9\ nm$
D_I	$= 2.6 \cdot 10^{-7}\ cm^2.sec^{-1}$
C_I^{eq}	$= 1.9 \cdot 10^{13}\ cm^{-3}$

The model is similary to the Grove model. The deviation from the Grove model is given by two exponential expressions, that calculate the excess of oxidation rate in thin oxide layers. For the simulation of the kinetics of interstitial supersaturation we need the oxide growth rate as a function of time. Therefore (17) was also solved in ZOMBIE. The simulation was calculated at 1000°C with parameter values given in table 2. Fig.9 shows the oxide thickness during the first 100 minutes at a temperature of 1000°C for dry oxidation:

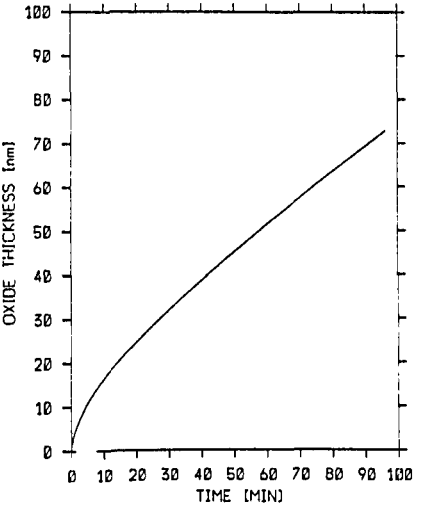

Fig.9

3.2 Generation Model of Interstitials.

The interstitials are produced during thermal oxidation because a fraction θ of silicon atoms at the interface is not oxidised. Therefore the generation rate of interstitials (G_I) during thermal oxidation can be written as

$$G_I = \theta \cdot C_{ox} \cdot \frac{\partial x_{ox}}{\partial t} \qquad (18)$$

C_{ox} denotes the number of molecules/cm^3 of silicon dioxide ($2.2 \cdot 10^{22} cm^{-3}$) The generation term given in (18) is now inserted in (13). With ZOMBIE the numerical solution of the oxide growth rate, the interstitial concentration and the average supersaturation can be obtained. The results of the simulations are given in Fig.10 and Fig.11. These plots show C_I/C_I^{eq} and the average supersaturation at the SiO_2-Si interface. By variation of the surface recombination velocity (K_I) the plots of the interstitial surface concentration and their average supersaturation change their shape. A change of θ does not change the shape of the curves. θ only alters the number of produced interstitials. In many cases a stationary generation rate of interstitials is assumed /1,9/. This stationary generation rate can be obtained by setting $J_I=0$ at x=0 in (13). One obtains ($\theta/K_I = 5 \cdot 10^2$ is kept constant)

$$C_I = \frac{G_I}{K_I} + C_I^{eq} \qquad (19)$$

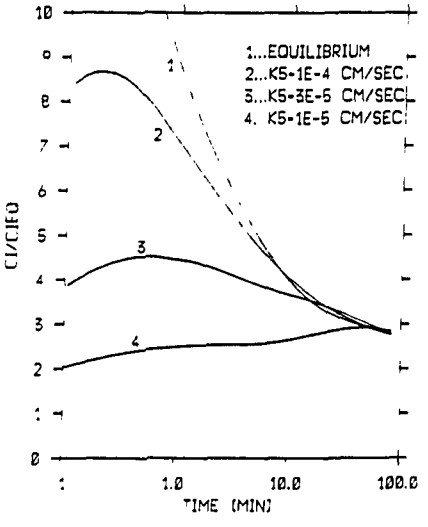

Fig.10

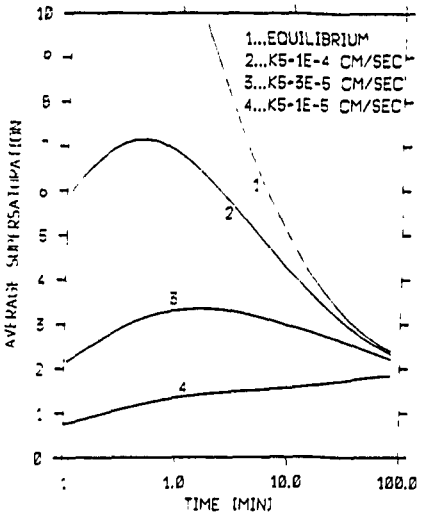

Fig.11

Curve 1 in the Fig.10 to Fig.11 shows this "dynamical equilibrium" behaviour. The other curves (2 to 4) approach to the equilibrium curve after long times. In the curves 2 to 4 the surface recombination velocity and ϑ were chosen lower. Yet the ratio of ϑ/K_I was the same as in curve 1. The curves 2 to 4 show a similar behaviour: at t=0 no supersaturation exists. At the beginn of the oxidation there is a high generation rate of interstitials and supersaturation increases. With advancing time supersaturation approaches to dynamical equilibrium. The curves 2 and 3 of Fig.11 show the supersaturation range which is typical for OED experiments.
Finally we have plotted the dynamical equilibrium of the average supersaturation of interstitials as shown in Fig.12. This curve reveals a $t^{-0.25}$ dependence in the range of 100 to 1000 min as found in the experiments /1,3,8/. Therefore this dependence can be obtained by a consistent physical model for interstitial generation. For the curves without the dynamical equilibrium we can chose the parameters in a way that they show the same behaviour in the range from 100 to 1000 min as the curve in Fig.12.
A more realistic physical model for the interstitial supersaturation must take account of the bulk recombination and diffusion of interstitials and vacancies.

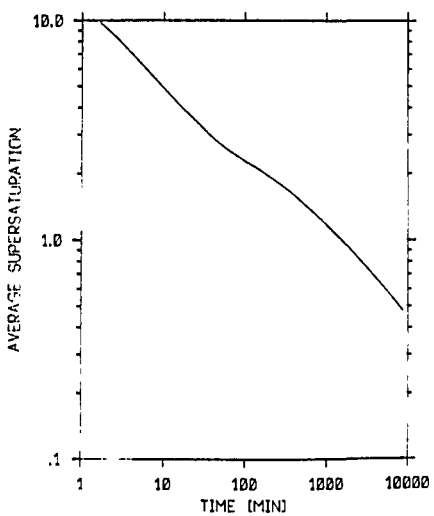

Fig.12

4. THE INTERSTITIAL AND VACANCY MODEL

The continuity equation for vacancies and interstitials is given by

$$\frac{\partial C_I}{\partial t} = D_I \cdot \frac{\partial^2 C_I}{\partial x^2} - k_B \cdot (C_I \cdot C_V - C_I^{eq} \cdot C_V^{eq}) \qquad (20)$$

$$\frac{\partial C_V}{\partial t} = D_V \cdot \frac{\partial^2 C_V}{\partial x^2} - k_B \cdot (C_I \cdot C_V - C_I^{eq} \cdot C_V^{eq}) \qquad (21)$$

The second term in (20) and (21) is the bulk recombination term between interstitials and vacancies. K_R is the recombination coefficient and depends only on temperature. C_I^{eq} and C_V^{eq} are their equilibrium values. The used initial and boundary conditions are

$$C_I = C_I^{eq}, \quad C_V = C_V^{eq} \quad \text{for } t=0 \qquad (22.a)$$

$$J_I = G_I - K_I \cdot (C_I - C_I^{eq}) \quad \text{for } x=0 \qquad (22.b)$$

$$J_V = - K_V \cdot (C_V - C_V^{eq}) \quad \text{for } x=0 \qquad (22.c)$$

$$J_I = 0 \quad \text{and} \quad J_V = 0 \quad \text{for } x=150\mu m \qquad (22.d)$$

The values of the parameters for interstitials, vacancies and K_R are given in table 2 and 3.

TABLE 3

Parameter values for the vacancies and bulk recombination coefficient at 1000°C /8,10/.

D_V	$= 1.2 \cdot 10^{-9}$ cm^2.sec^{-1}
C_V^{eq}	$= 2.4 \cdot 10^{15}$ cm^{-3}
K_R	$= 10^{-17}$ cm^3.sec^{-1}

The average supersaturation of vacancies $\langle \Delta CV \rangle$ can be defined similar to the avarage supersaturation of interstitials (10).

Furthermore ZOMBIE uses a similar equation for $\langle \Delta CV \rangle$ as for $\langle \Delta C_I \rangle$ in (14). Fig.13 and Fig.14 show typical profiles of $\langle \Delta C_I \rangle$ and $\langle \Delta C_V \rangle$ at different times. the curves 1 to 4 in Fig.13 indicate a gradually increase of the supersaturation of I whereas the curves 1 to 4 in Fig.14 show a simultaneous decrease of V. The deviation of V from its equilibrum value advances into the depth with increasing time.

For thermal oxidation experiments it is important to know the average supersaturation of interstitials and vacancies at the surface. Fig.15 and Fig.16 show the behaviour of $\langle C_I \rangle$ and $\langle C_V \rangle$ at the silicon surface. A reasonable bulk recombination coefficient K_R (10^{-17} cm^{-3} sec^{-1}) /10/ has been chosen for the simulation of the curves in Fig.15 and Fig.16. We have also chosen $K_V = K_I = K_S$. In Fig.15 the curves 1 to 5 have the same shape up to $t = 4 \cdot 10^3$ sec. In this region these curves have approximately the same behaviour as the curves in Fig.11. From $t = 4 \cdot 10^3$ sec on the shape of the curves differ from one another. For lower values of K_S (curve 1 and 2) the interstitial supersaturation increases continuously (fill-up effect). On the other hand the vacancy undersaturation in Fig.16 is stronger for lower values of K_S. The next point was the simulation of the behaviour of $\langle \Delta C_I \rangle$ and $\langle \Delta C_V \rangle$ at the backside (x=300µm). Furthermore we have examined the dependence of $\langle \Delta C_I \rangle$ and $\langle \Delta C_V \rangle$ on K_S in Fig.17 and Fig.18. It takes the interstitials a certain extent of time until they reach the backside because the interstitials have to remove the vacancies by bulk recombination. Similar to the surface Fig.17 shows the fill-up effect for the same values of K_S. So for $t > 10^4$ sec the shape of the curves on the surface are similar to the backside in the Fig.15 to Fig.18.

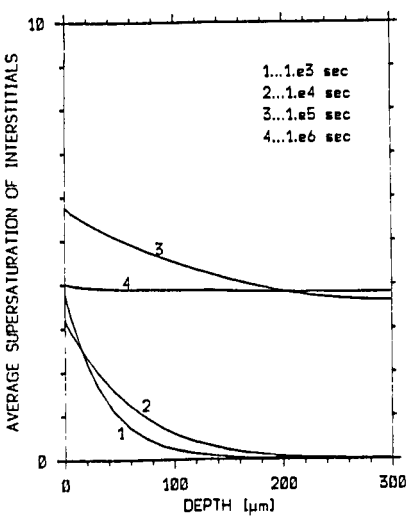

Fig.13

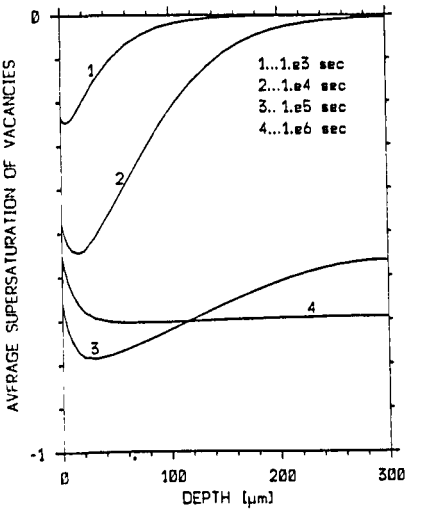

Fig.14

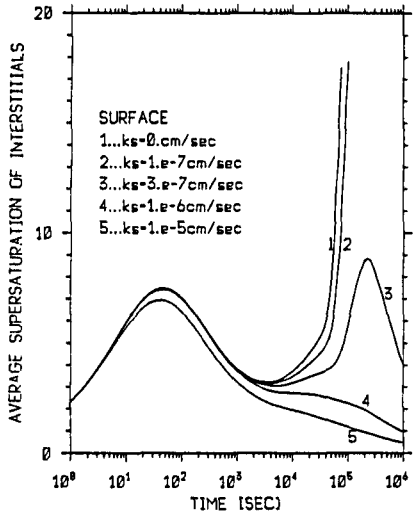

Fig.15

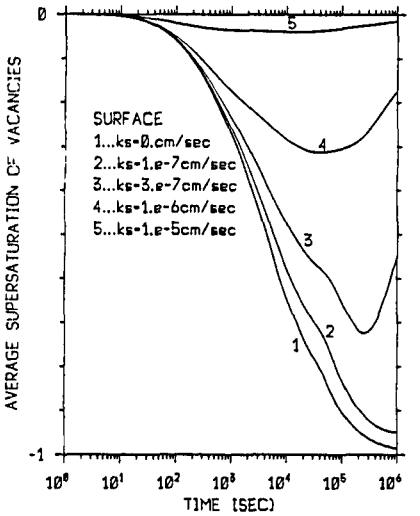

Fig.16

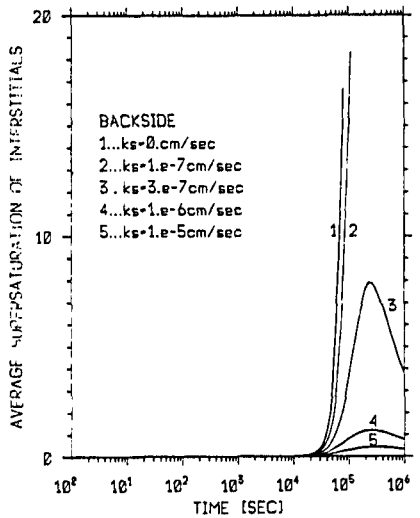

Fig.17

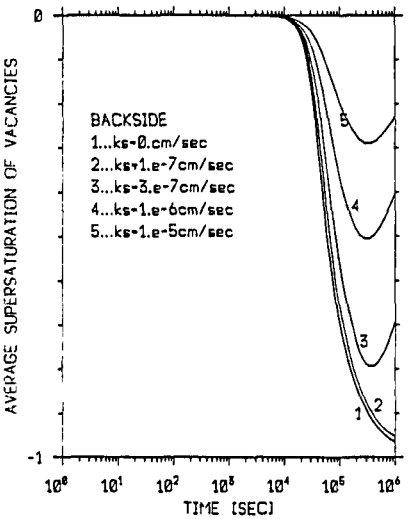

Fig.18

5. CONCLUSION

In summary we can conlude:

1) ZOMBIE is a very flexibel programm package and powerful for problem solving in the fields of diffusion.

2) It is possible to obtain $\langle C_I \rangle$ proportional to $t^{-0.25}$ in the from experiment known range assuming G_I to be proportional to the oxidation rate.

3) It has exposed that it is necessary to take account of C_V and C_I in order to obtain a more realistic result.

4) The simulation in this work has shown that the surface recombination velocity and the bulk recombination have a strong influence on the behaviour of V and I.

REFERENCES

1. ANTONIADIS, D.A. and MOSKOWITZ, I. "Diffusion of Substitutional Impurities in Silicon at Short Oxidation Times: An Insight into Point Defect Kinetics" J. Appl. Phys. Vol. 53, p.6788, 1982.
2. MIZUO, S. and HIGUCHI, H. "Effect of Back-Side Oxidation on B and P Diffusion in Si Directly Masked with Si_3N_4 Films" J. Electrochem. Soc. Vol. 129, p.2292, 1982.
3. FAHEY, P.M. "Point Defects and Dopant Diffusion in Silicon" Dissertation, Stanford University, Stanford, CA 94305, 1985.
4. HU, S.M. "Kinetics of Interstitial Supersaturation During Oxidation of Silicon" Appl. Phys. Lett. Vol. 43, p.449, 1983.
5. GROVE, A.S. "Physics and Technology of Semiconductor Devices" John Wiley and Sons, Inc., New York, London, Sydney, 1967.
6. YEAGER, H.R. and DUTTON, R.W. "An Approach to Solving Multiparticle Diffusion Exhibiting Nonlinear Stiff Coupling" IEEE Trans. on Computer-Aided Design, Vol. CAD-4, p.408, 1985.
7. MASSOUD, H.Z., HO, C.P. and PLUMMER, J.D. "Thin Oxide Growth Kinetics in Dry Oxygen", In:Final Report for Period 15 February 1981-31 March 1982. Integrated Circuits Laboratory, Standford University, Standford, CA 94305, p.194, 1982.
8. GOESELE, U. and TAN, T.Y. "The Influence of Point Defects on Diffusion and Gettering in Silicon", presented by M.R.S.-Meeting in Boston, 1984.
9. GOESELE, U. and TAN, T.Y. "The Role of the Vacancies and Self-interstitials in Diffusion and Agglomeration Phenomena in Silicon", In: Proceedings of the Satellite Symposium to ESSDERC'82, MUNICH(Ed. E. Sirtl et. al), The Electrochem. Soc. Inc. (U.S.A), p.17, 1983.
10. GUERRERO, E. O. "Verteilung von Dotierungsatomen in Silizium-Einkristallen" Dissertation, Technical University of Vienna, Vienna, Austria, 1984.

ACKNOWLEDGEMENT

This work has been supported by the Fonds zur Förderung der wissenschaftlichen Forschung(project no. S43/10). The authors wish to thank the research laboratories of SIEMENS AG at Munich, FRG. Furthermore we also wish to acknowledge Dr. Fahey for helpful discussions.